

MEC-Based Modelling of Claw Pole Machines: Application to Automotive and Wind Generating Systems

Amina Ibala, Rabeb Rebhi, Ahmed Masmoudi[‡]

* Research Unit on Renewable Energies and Electric Vehicles

University of Sfax, Sfax Engineering School, P.O. Box W, 3038 Sfax, Tunisia

[‡]Corresponding Author; Tel: +216 98 906 117, Fax: +216 74 275 595, e-mail: a.masmoudi@enis.rnu.tn,
kam-ali@lycos.com, fbouchafa@gmail.com

Received : 03.10.2011 Accepted: 06.10.2011

Invited Paper

Abstract- The paper deals with the development and the finite element validation of the magnetic equivalent circuits (MECs) of three claw pole topologies. These are considered as viable candidates for automotive and wind generating applications. The first concept is the conventional claw pole alternator, the second claw pole topology has a DC-excitation winding in the stator, rather than in the rotor in conventional machine, and the third claw pole concept is a one-phase machine with claw pole in the stator and PM excitation in the rotor. The proposed MECs consider both no-load and loaded armature operations. It also accounts for the saturation of the magnetic circuit. The resolution of the established MECs is carried out using the *Newton-Raphson* algorithm. A validation of the proposed MECs is achieved considering a comparison between their results and those yielded by 3D finite element analysis.

Keywords- claw pole machine; automotive and wind generating systems; magnetic equivalent circuit; Newton-Raphson algorithm; validation; finite element analysis.

1. Introduction

In recent years, many efforts have been focused upon the modelling of new topologies of electric machines. The major reported solutions consider analytical models which are generally validated by finite element analysis (FEA) or by experiments of by both. The most considered analytical model is the one based on the magnetic Ohm law, leading to the magnetic equivalent circuit (MEC).

The increasing interest in MECs is due to the low CPU-time required for their resolution, which represents a crucial issue especially with the topological complexity of novel machines.

One of the complex topologies is the claw pole generator; commonly integrated in automotive power generating systems. Its popularity is mainly

due to the heteropolar topology of its rotor which offers the possibility of integration of a high pole pair number in a low volume leading to interesting generation capabilities.

Other claw pole topologies are currently given an increasing attention as far as they could be integrated in other applications, such as wind generating, hybrid propulsion systems of road vehicles, and so on.

Within this trend, the present paper is devoted to the MEC modelling of three claw pole concepts, which are:

- Concept with claw poles and DC excitation in the rotor [1,2,3,4].
- Concept with claw poles in the rotor and a DC excitation in the stator [5].

➤ Concept with claw poles in the stator and a PM excitation in the rotor [6,7,8], which could be integrated in wind generating systems.

A numerical procedure based on the *Newton-Raphson* algorithm is proposed for the resolution of the proposed MECs. Finally, a validation of the proposed MECs is carried out considering a comparison MEC/FEA.

2. Description and Flux linkage of the Studied Claw Pole Concepts

2.1. Concept with Claw Poles and DC Excitation in the Rotor

The first claw pole concept exhibits the same topology as the conventional claw alternator. Fig. 1 shows a layout of such a concept.

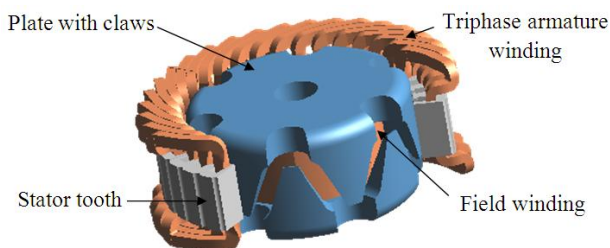


Fig. 1. Layout of the first claw pole concept.

Figure 2 illustrates the main flux path through the magnetic circuit of the first concept. Such a path is described as follows:

- axially in the rotor magnetic circuit part surrounding the shaft
 - radially in the rotor north plate
 - axially and radially in the north rotor claws
 - radially in the air gap to the stator teeth
 - circumferentially in the stator yoke
 - radially in the air gap
 - axially and radially in the two adjacent south claws
 - radially in the rotor south plate
 - axially in the rotor magnetic circuit part surrounding the shaft

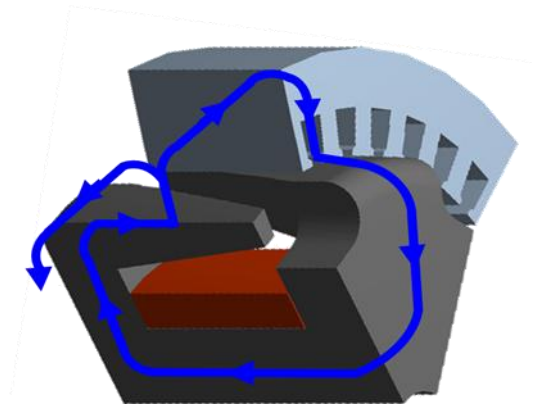


Fig. 2. Main Flux path through the magnetic circuit of the first claw pole concept.

2.2. Concept with Claw Poles in the Rotor and a DC Excitation in the Stator

Figure 3 shows an exploded view of the second claw pole concept.

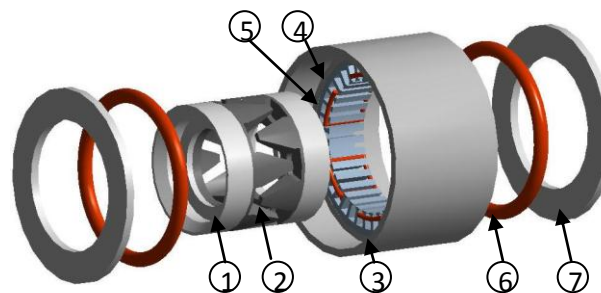


Fig. 3. Exploded view of the second claw pole concept. Legend: (1) magnetic ring, (2) claws, (3) stator yoke, (4) lamination, (5) armature winding, (6) field winding, (7) magnetic collector.

The flux linkage between stator and rotor in the second claw pole concept is characterized by two types of paths, such that:

- 2D flux paths which are considered as homopolar leakage fluxes
- 3D flux paths which represent the useful flux. These are illustrated in Fig. 4 and are described as follows:
 - axially in the stator yoke
 - radially down through the magnetic collector and the first lateral air gap
 - radially then axially in the magnetic ring
 - axially and radially in the north claws
 - radially up in the main air gap and in the stator teeth

- circumferentially in stator laminations
- radially down in the stator teeth and the main air gap
- axially and radially in the two adjacent south claws
- axially then radially in the magnetic ring
- radially up through the second lateral air gap and the magnetic collector on the other side of the machine.

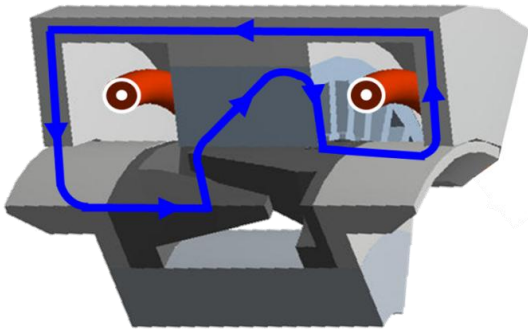


Fig. 4. Main Flux path through the magnetic circuit of the second claw pole concept.

2.3. Concept with Claw Poles in the Stator and a PM Excitation in the Rotor

Figure 5 shows an exploded view of the third claw pole concept. It could be integrated in wind generating systems [12].

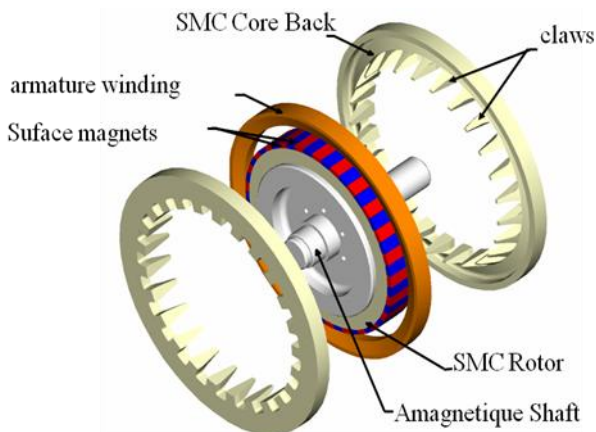


Fig. 5. Exploded view of the third claw pole concept.

Figure 6 illustrates the main flux path through the magnetic circuit of the third concept. Such a path is described as follows:

- axially in the stator core back
- radially down through the stator flanks

- axially and radially in the stator claws
- radially down in the air gap then the rotor PMs
- circumferentially in the rotor core back
- radially up in the adjacent magnets then in the air gap
- axially and radially in the adjacent claws,
- radially up through the stator flanks to close the loop in the stator core back

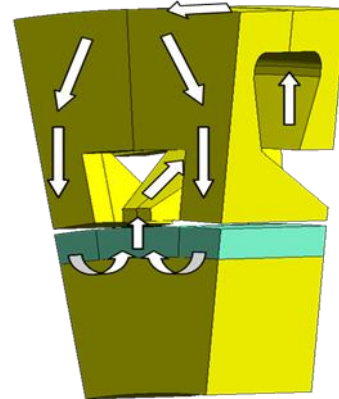


Fig. 6. Main Flux path through the magnetic circuit of the third claw pole concept.

3. MEC Based Modelling of the Claw Pole Concepts

The derivation of the MECs of the three presented claw pole topologies is based on the above- described flux paths. Taking into account the directions of the fluxes in the different parts of the magnetic circuit and the corresponding materials, one can define the reluctances of the MEC. The fluxes are the results of the applied MMFs.

3.1. Expressions of the Reluctances

In the case of linear materials, the reluctance of a part of the magnetic circuit is expressed as follows:

$$R = \frac{1}{\mu_0 \mu_r} \frac{L}{S} \quad (1)$$

where μ_0 is the permeability in the air, μ_r is the relative permeability, L is the flux path average length and S is the section area.

In the case of saturated material, the reluctance turns to be non-linear function of the flux, such that:

$$R = \frac{L}{\Phi} H \left(\frac{\Phi}{S} \right) \quad (2)$$

where Φ is the magnetic flux and $H(B)$ is the analytical expression of the magnetic field H versus the flux density B , which is expressed as follows:

$$B = \frac{\Phi}{S} \quad (3)$$

3.2. MECs of the Claw Pole Concepts

Figures 7, 8 and 9 show respectively the proposed MECs of the first, the second and the third claw pole topologies, where the saturation as well as the armature magnetic reaction are taken into account.

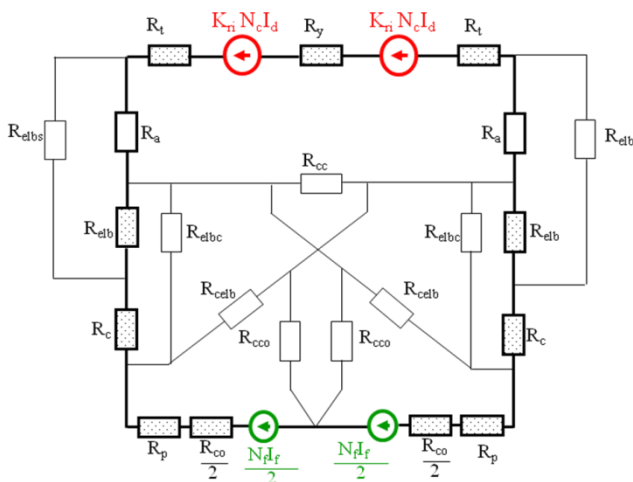


Fig. 7. MEC of the first claw pole concept.

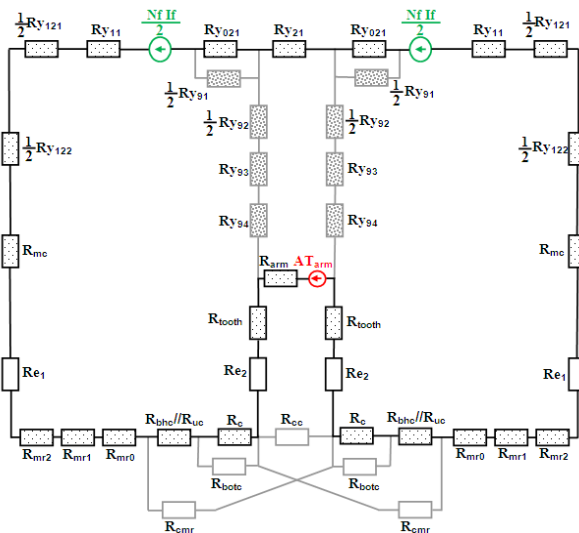


Fig. 8. MEC of the second claw pole concept.

4. Numerical Procedure to Solve the MECs of the Claw Pole Concepts

4.1. Case of no- Load Operation

In a first step, the resolution of the proposed MECs treats the no-load operation. Generally speaking, if a network includes b reluctances and n nodes, the number of independent loops is equal $m=b-n+1$.

Let us consider, for instance, the MEC of the first claw pole concept, shown in Fig. 10, where the orientation of branches and the loops are indicated.

One can notice that the MEC includes 18 branches and 9 nodes. Therefore, the resolution of the network can be reduced to 10 independent loops, as illustrated in Fig. 10.

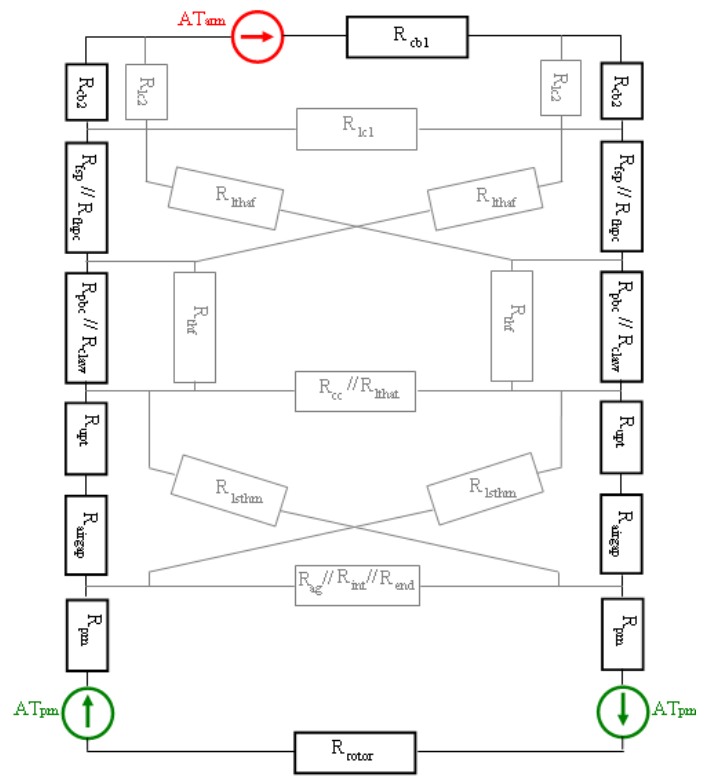


Fig. 9. MEC of the third claw pole concept.

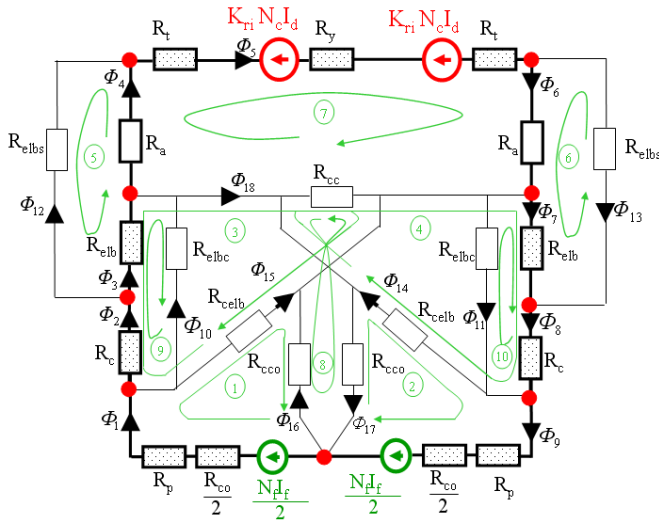


Fig. 10. MEC of the first claw pole concept where the orientations of the branches and the loops are indicated.

Referring to the literature [10,11], it has been reported that numerical procedures based on the *Newton-Raphson* algorithm are suitable to achieve the resolution of the MECs of claw pole machines, leading to accurate results.

The *Newton-Raphson* procedure is based on the loop matrix S , which in the case of the first claw pole concept is expressed as follows:

$$S = \begin{pmatrix} 1 & 0 & 0 & 0 & 0 & 0 & 0 & 0 & 0 & 0 & 0 & 0 & 0 & 0 & 0 & 1 & -1 & 0 & 0 \\ 0 & 0 & 0 & 0 & 0 & 0 & 0 & 0 & 0 & 1 & 0 & 0 & 0 & 0 & 0 & -1 & 0 & 0 & -1 \\ 0 & 1 & 1 & 0 & 0 & 0 & 0 & 0 & 0 & 0 & 0 & 0 & 0 & 0 & 0 & -1 & 0 & 0 & 1 \\ 0 & 0 & 0 & 0 & 0 & 0 & 0 & 1 & 1 & 0 & 0 & 0 & 0 & 0 & 0 & 1 & 0 & 0 & 0 & 1 \\ 0 & 0 & 1 & 1 & 0 & 0 & 0 & 0 & 0 & 0 & 0 & 0 & -1 & 0 & 0 & 0 & 0 & 0 & 0 & 0 \\ 0 & 0 & 0 & 0 & 0 & 0 & 1 & 1 & 0 & 0 & 0 & 0 & 0 & 0 & -1 & 0 & 0 & 0 & 0 & 0 \\ 0 & 0 & 0 & 0 & 1 & 1 & 1 & 0 & 0 & 0 & 0 & 0 & 0 & 0 & 0 & 0 & 0 & 0 & 0 & -1 \\ 0 & 0 & 0 & 0 & 0 & 0 & 0 & 0 & 0 & 0 & 0 & 0 & 0 & 0 & 0 & 0 & 1 & 1 & -1 & -1 \\ 0 & 1 & 1 & 0 & 0 & 0 & 0 & 0 & 0 & 0 & -1 & 0 & 0 & 0 & 0 & 0 & 0 & 0 & 0 & 0 \\ 0 & 0 & 0 & 0 & 0 & 0 & 0 & 0 & 0 & 0 & 0 & 0 & 0 & 0 & 0 & 0 & 0 & 0 & 0 & 0 \end{pmatrix}$$

where S_{ij} is equal to:

- 0 in the case where the flux of branch j is not included in loop i ,
- 1 in the case where the flux of branch j is in the same direction of the orientation of loop i ,
- -1 in the case where the flux of branch j is in the opposite direction of the orientation of loop i .

The vector of the MMFs F of the different loops, correctly oriented, is built as well as the diagonal reluctance matrix R [5,9]. The magnetic *Ohm* law expressed for the MEC branches yields:

$$U = R\Phi \quad (4)$$

where U and Φ are the branch MMF and flux vectors, respectively.

Thanks to the topological matrix S , one can obtain the loop MMF vector F as follows:

$$F = SU \quad (5)$$

The node law yields:

$$\Phi = S^T \Psi \quad (6)$$

where Ψ is the vector of loop fluxes.

Combining Eq. (4) and Eq. (5) yields:

$$F = SR\Phi \quad (7)$$

Considering Eq. (6), and in the case of non saturated magnetic circuit, the loop fluxes are calculated as follows:

$$\Psi = (SRS^T)^{-1}F \quad (8)$$

However in the case of saturated materials, the reluctances depend on the fluxes which are nonlinear. As a result, the inverse of matrix SRS^T cannot be calculated. In order to solve this problem, a vector C is introduced, such that:

$$C = F - SRS^T \Psi \quad (9)$$

The resolution of the reluctant model is achieved when all elements of vector C turn to be null.

The MEC resolution enables the assessment of the fluxes circulating in the different parts of the magnetic circuit and the computation of the no-load back-EMF, which is expressed as follow:

$$E = \frac{1}{\sqrt{2}} N_a \omega \Phi_m \quad (10)$$

where N_a is the number of turns per armature phase, ω is the angular frequency and Φ_m is the maximum flux crossing a phase which is assessed using the MEC.

4.2. MEC Resolution Under Load Operation

The resolution of the MECs could be extended to the case of load operation. Claw pole topologies are considered as salient so that including the effect of the armature magnetic reaction in both q-

and d-axis is necessary. This said, it is generally assumed that the saturation along the q-axis is negligible compared to the d-axis one. Therefore, a constant stator transverse inductance is defined.

The magnetic circuit parts located in the d-axis are saturated, so that the corresponding reluctances turn to be a nonlinear function of the fluxes. Then, a MEC accounting for the d-axis armature reaction is considered in order to find out the flux through the involved parts of magnetic circuit. Of particular interest is the linkage flux which allows the determination of the d-axis component of the back-EMF using Eq. (10).

The armature magnetic reaction in the d-axis is modelled by the MMF, coloured in red in the MECs of three claw pole concepts. Such MMF produces a flux circulating through the magnetic circuit in an opposite direction to the one of the field flux.

Under load operation, the back-EMF phasor could be expressed in terms of its d- and q-components, as follows:

$$\bar{E} = \bar{E}_d + \bar{E}_q \quad (11)$$

$$\begin{cases} \|\bar{E}_d\| = E_d(I_f, I_d) \\ \|\bar{E}_q\| = L_q \omega I_q \end{cases} \quad (12)$$

where I_d and I_q are the armature current d- and q-components, and where I_f is the field current.

Furthermore referring to *Blondel* model, the back-EMF can be expressed as follows:

$$\bar{E} = R\bar{I} + \bar{V} + j l_\sigma \omega \bar{I} \quad (13)$$

where :

- \bar{I} and \bar{V} are the armature current and voltage phasors, respectively;
- R and l_σ are the phase resistance and leakage inductance, respectively.

Combining both expressions of the back-EMF, one can draw the phasor diagram of the loaded claw pole machine, considering the case of a resistance in the armature, as illustrated in Fig. 11.

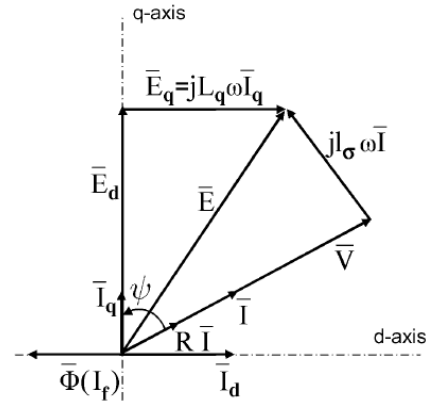


Fig. 11. Phasor diagram of the claw pole machine in the case of a resistive load.

Referring to Fig. 11, and accounting for Eq. (11) and Eq. (13), one can establish the armature equations within the d- and q-axis, as follows:

$$\begin{cases} RI \cos(\psi) + l_\sigma \omega I \sin(\psi) - E_d = 0 \\ -RI \sin(\psi) + l_\sigma \omega I \cos(\psi) + E_q = 0 \end{cases} \quad (14)$$

where both ψ and E_d are functions of the linkage flux which is calculated using the MEC, according to the numerical procedure whose bloc diagram is shown in Fig. 12.

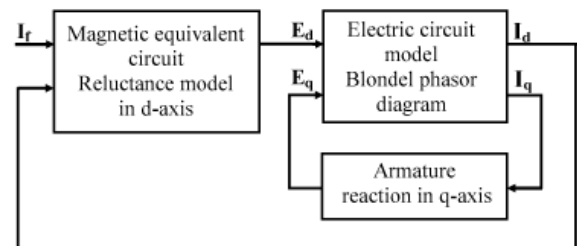


Fig. 12. Block diagram of the numerical procedure developed for the resolution of MEC in the case of load operation.

5. Case Study

A comparison between the results yielded by the MECs and the ones computed by finite element method (FEM), considering the three claw pole concepts, is treated in this section. The comparison is focused upon the back-EMF at no-load operation which is plotted versus the field current for the first and the second topologies. The obtained results are illustrated in Fig. 13 and in Fig. 14.

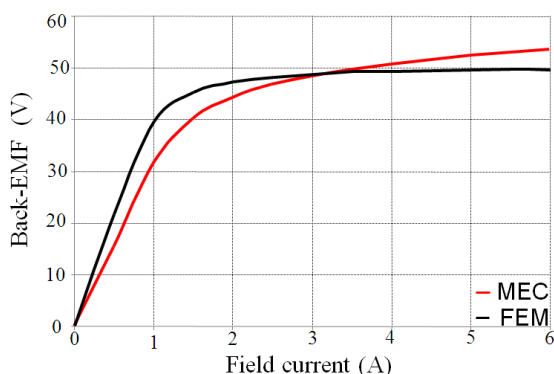


Fig. 13. First claw pole concept Back-EMF versus the field current under no-load operation for a speed of 1000 rpm.

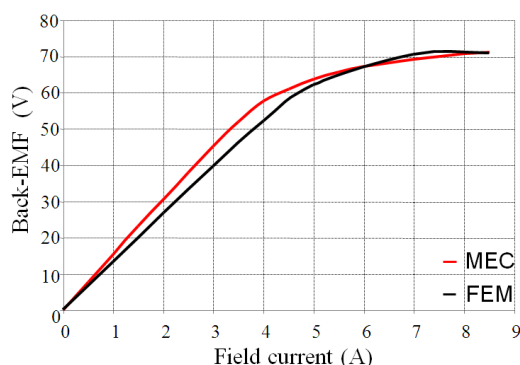


Fig. 14. Second claw pole concept Back-EMF versus the field current under no-load operation for a speed of 1000 rpm.

Concerning the third claw pole topology, the core-back flux for different ampere-turns has been the subject of the comparative study. The obtained results are shown in Fig.15.

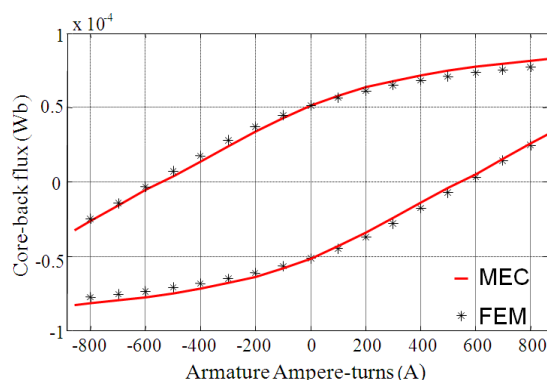


Fig. 15. Third claw pole concept core-back flux versus armature Ampere-turns.

Referring to Fig. 13, Fig. 14 and Fig. 15, one can clearly notice the agreement between the results yielded by the MECs and those computed by FEM in both linear and saturated operating regions.

6. Conclusion

The paper was aimed at the principle of operation and the modelling of three claw pole topologies. These could be integrated in automotive and wind generating systems. First, an analysis of the flux paths through the magnetic circuits of the treated concepts was presented and analysed. Then a general approach to build up the magnetic equivalent circuit (MEC) of a claw pole concept was proposed. Following the establishment of the MECs of the three claw pole concepts under study, a numerical procedure based on the *Newton-Raphson* algorithm allowed the resolution of the proposed MECs, leading to an assessment of the fluxes circulating in the different parts of the magnetic circuit.

A comparison between the results yielded by the MEC and those computed by the FEM, was focused on the no-load back-EMF in the case of the first and second claw pole concepts. The core-back flux versus the armature ampere-turns has been the subject of the comparison between the results of the MEC and those yielded by the FEM.

It has been found that the results obtained following the resolution of the proposed MECs are in agreement with those computed by the FEM.

Acknowledgements

The works related to the third claw pole machine have been developed in the Newcastle Electric Drives and Machines Group of the University of Newcastle Upon Tune under the supervision of Prof. Alan. G. Jack.

References

- [1] M. Hecquet and P. Brochet "Modeling of a claw-pole alternator using permeance network coupled with electric circuits," *IEEE Transactions on Magnetics*, Vol. 31, No. 3, pp. 2131-2134, 1995.
- [2] S. Kuppers and G. Henneberger, "Numerical procedures for the calculation and design of automotive alternators," *IEEE Transactions on Magnetics*, Vol. 33, No. 2, pp. 2022 – 2025, 1997.
- [3] S. H. Lee, S. O. Kwon, J. J. Lee, and J. P. Hong, "Characteristic Analysis of Claw-Pole Machine Using Improved Equivalent Magnetic Circuit," *IEEE Transactions on Magnetics*, Vol. 45, No. 10, pp. 4570-4573, Octobre 2009.

- [4] L. Li, A. K. Lebouc, A. Foggia, and J. C. Mipo, "Influence of magnetic materials on claw pole machines behavior," *IEEE Transactions on Magnetics*, vol. 46, no. 2, pp. 574-577, 2010.
- [5] A.G. Jack. "Experience with the use of soft magnetic composite in electrical machines," *Proc. of the International Conference on Electrical Machines*, vol. 3, pp. 1441-1448, Istanbul-Turkey, September 1998.
- [6] P. G. Dickinson, A. G. Jack and B. C. Mecrow, "Improved permanent magnet machines with claw pole armatures," *CD-ROM of the International Conference on Electrical Machines*, Bruges-Belgium, August 2002.
- [7] A. Ibala and A. Masmoudi, "Accounting for the Armature Magnetic Reaction and Saturation Effects in the Reluctance Model of a New Concept of Claw-Pole Alternator," *IEEE Transactions on Magnetics*, Vol. 46, No. 11, pp. 3955-3961, November 2010.
- [8] A. Ibala, A. Masmoudi, G. Atkinson, and A.G. Jack, "On the modeling of a TFPM by reluctance network including the saturation effect with emphasis on the leakage fluxes," *COMPEL*, Vol. 30, No. 1, pp. 151-171, 2011.
- [9] A. Ibala, Elaboration and validation of the MECs of different claw pole machines (in French), PhD Thesis, *Sfax Engineering School*, Sfax, Tunisia, 2011.
- [10] A. Deale, L. Albert, L. Gerbaut et F. Wurtz. Automatic generation of sizing models for the optimization of electromagnetic devices using reluctance networks. *IEEE Trans. Magn.*, vol. 40, no. 2, pp. 830-833, 2004.
- [11] L. Albert, Modelling and optimization of claw pole alternators applied to automotive systems (in French), PhD Dissertation, *Institut National Polytechnique de Grenoble*, France, 2004.
- [12] B. Multon. Wind Energy and Electrical Engineering (in French), *STIM Doctoral School Conference*, Saint-Nazaire, France, October 2002.